



APPLICATION OF THE SPECIFIC BARRIER MODEL TO THE SEISMIC FRAGILITY ASSESSMENT OF CRITICAL FACILITIES

A. Wanitkorkul¹, B. Halldorsson², A. S. Papageorgiou³, and A. Filiatrault⁴

ABSTRACT

This paper presents the results of a numerical study on the influence of structural passive supplemental damping systems on structural and nonstructural seismic fragilities of a critical facility. Hysteretic and viscous damping systems are used to retrofit a 4-story steel framed prototype building assumed to be part of an acute care facility which contains different types of secondary nonstructural systems attached at various levels of the building. The recently calibrated Specific Barrier Model (SBM) is used to simulate four different ensembles of synthetic strong ground motions for a hypothetical site located on the west-coast of the United States. Each ensemble is representative of a different seismic hazard level at the site. Nonlinear dynamic analyses are performed to generate fragility curves for the structural system and nonstructural components based on various performance objectives. The performance of each passive supplemental damping system in reducing the seismic fragilities of both structural and nonstructural components is evaluated.

Introduction

To achieve a given target seismic performance level for critical facilities, such as acute care facilities, the harmonization of the performance levels between structural and nonstructural components and systems is required. Even if the structural components of a building achieve an immediate occupancy performance level during a seismic event, failure of nonstructural components inside the building can lower the performance level of the entire building. In comparison to structural components and systems, there is still relatively limited information on the seismic performance of building nonstructural components. Basic research work in this area has been sparse, and the available codes and guidelines are usually, for the most parts, based on past experiences, engineering judgment, and intuition, rather than on experimental and analytical results.

¹Post-doctoral Research Associate, Dept. of Civil, Structural, and Environmental Engineering, University at Buffalo, State University of New York, Buffalo, NY 14260, USA

²Former Ph.D. Candidate, Dept. of Civil, Structural, and Environmental Engineering, University at Buffalo, State University of New York, Buffalo, NY 14260, USA

³Professor, Dept. of Civil Engineering, University of Patras, Patras 26500, Greece

⁴Professor, Dept. of Civil, Structural, and Environmental Engineering, University at Buffalo, State University of New York, Buffalo, NY 14260, USA

This study investigates numerically the influence of passive hysteretic and viscous damping systems on structural and nonstructural seismic fragilities of a 4-story prototype steel framed building assumed to be part of an acute care facility containing three different types of secondary nonstructural systems attached at various levels of the building. The recently calibrated Specific Barrier Model (Halldorsson 2004) is used to simulate four different ensembles of synthetic strong ground motions for a hypothetical hospital site located on the west-coast of the United States. Each ensemble is representative of a different seismic hazard level at the site. Nonlinear dynamic analyses are used to generate fragility curves for the structural system and nonstructural components based on various performance objectives. The performance of each passive damping system in reducing the seismic fragility of both structural and nonstructural systems is evaluated.

Building Structure and Modeling

A particular prototype 4-story steel frame building part of a hypothetical acute care facility located in Southern California is considered for analyses. It is assumed that the facility was constructed in the early 1970s and conforms to the seismic requirements of that era (ICBO 1970). The seismic frames are assumed to be constructed with ASTM A572 and A588 Grade 50 steel. ASTM A36 steel is considered for all remaining structural elements. Gravity loads acting on the structure consist of 5.7 kPa from the floor dead load, 5.7 kPa from the roof dead load, 1.9 kPa from the floor live load, 1.0 kPa from the roof live load, and 0.8 kPa from the weight of the exterior walls. For seismic analyses, a live load reduction factor of 65% is applied to all floors except the roof level. Figure 1 illustrates the building model along with the corresponding member section numbers.

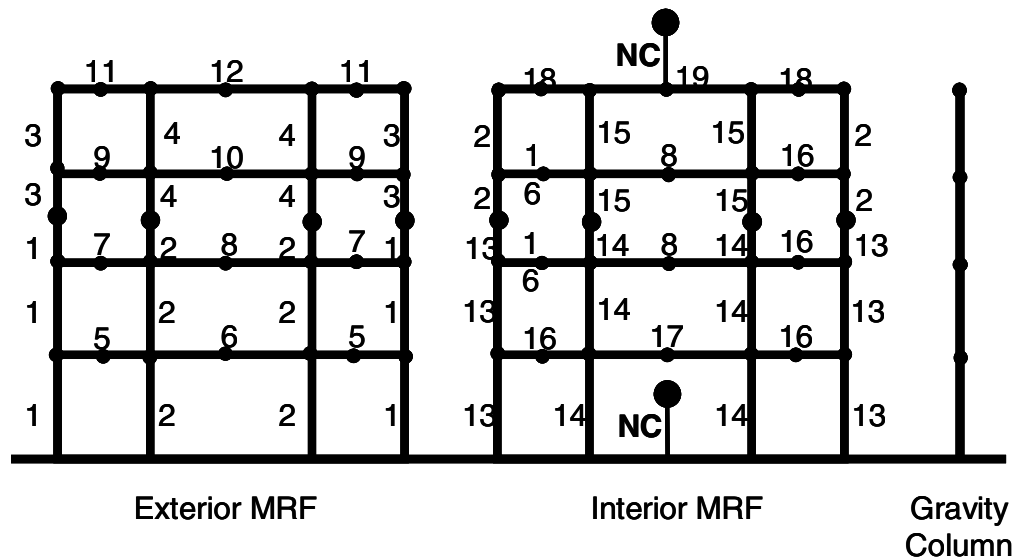


Figure 1. Building model and nonstructural components (NC).

Table 1 summarizes the steel sections for the various frame members. A bilinear moment-curvature hysteresis with 2% curvature hardening ratio was assigned to all frame members. To account for secondary (P- Δ) effects from the gravity frames, a pin-ended gravity column was included in the building model. This column carries all gravity loads from the gravity frames. It is constraint to have the same lateral floor displacements as those of the seismic frames.

Table 1. List of member sections.

Section No.	Designation	Section No.	Designation	Section No.	Designation
1	W 14x193	8	W 30x211	15	W 14x370
2	W 14x342	9	W 24x103	16	W 24x162
3	W 14x159	10	W 30x211	17	W 33x241
4	W 14x257	11	W 24x68	18	W 24x94
5	W 24x146	12	W 24x104	19	W 30x173
6	W 33x221	13	W 14x398		
7	W 24x131	14	W 14x455		

Modeling of Nonstructural Components

A single-degree-of-freedom system (spring-mass-dashpot) is used for modeling each of the three types of nonstructural components considered in this study, i.e. resonant, isolated, and sliding nonstructural components. The resonant nonstructural component is tuned to have its vibration period equal to that of the original building (0.76 sec) in order to represent the worst case scenario for the dynamic response of a nonstructural component rigidly anchored at its base. The isolated nonstructural component, on the other hand, is tuned to have a fundamental period of 2 sec. A linear elastic hysteresis model is assigned for these two types of nonstructural components. Finally, the sliding nonstructural component is modeled by a rigid-plastic hysteretic behavior with a coefficient of friction of 5%. A seismic weight of 100 kN is assumed for all three nonstructural component models. A dashpot element based on a damping ratio of 1% of critical is introduced for both the resonant and the isolated nonstructural components. No viscous damping is considered for the sliding nonstructural component since energy dissipation is assumed to be achieved by Coulomb-type friction only.

The three nonstructural component models are incorporated into the building model at two locations, i.e. the roof of the building and the base level. For each location, all three nonstructural components are assumed to be located at the center of the interior seismic frame, as illustrated in Fig. 1.

Performance Objectives

For structural fragilities, the performance objectives of the NEHRP seismic rehabilitation guidelines (ATC 2000) for inter-story drift limits were considered in this study, i.e. 0.7% for immediate occupancy, 2.5% for life safety, and 5% for collapse prevention performance level.

For nonstructural fragilities, no guidelines are currently available to associate peak response values with performance objectives. For illustration purposes in this study, minor, moderate, and severe damage to nonstructural components are associated with the absolute accelerations of 1.0 g, 2.0 g, and 7.0 g, respectively.

Retrofit Schemes

Two passive energy dissipation systems, hysteretic and viscous damping, are considered for retrofitting the structure. It is assumed that the damping devices are equipped with chevron brace elements installed in the mid-span in each story of the exterior seismic frame. A structural square tube of 356x356x16 mm (14x14x5/8 inch) is selected for all bracing members.

For the hysteretic dampers, the yield loads of the devices installed in the building are defined in term of the total yield shear (V_0) defined as a summation of the horizontal force components generated by each damper on each floor (Filiatrault *et al.* 2001). To evaluate the effects of various yield load distributions on structural and nonstructural fragilities, total yield shear normalized with total seismic weight (V_0/W) of 0.40, 0.60, and 0.80 are considered. These yield shears are equally distributed to each level of the building. Table 2 presents the resulting yield load values of each device on each floor level.

For the viscous dampers, three levels of equivalent first modal damping ratios are selected, i.e. 20%, 25%, and 30% of critical. The damping coefficients of each linear viscous damper at each floor level required to achieve these damping values are listed in Table 3. Details of the design procedure can be found elsewhere (e.g. Filiatrault *et al.* 2001).

Table 2. Yield loads: hysteretic damper Table 3. Damping coefficients: viscous dampers

V_0/W	Yield loads (kN)	
	Ground floor	Other floors
0.4	1548	1485
0.6	2322	2228
0.8	3097	2971

Floor	Damping coefficients (kN-sec/mm)		
	$\xi = 20\%$	$\xi = 25\%$	$\xi = 30\%$
Ground	18.3	22.8	27.4
2	17.8	22.3	26.8
3	15.9	19.9	23.8
4	12.0	15.0	18.0

Earthquake Ground Motions

Wanitkorkul and Filiatrault (2005) generated ensembles of synthetic strong ground motions for a hypothetical site in Southern California where the acute care building considered is assumed to be located. These synthetic motions were utilized in this study. These motions were generated based on four different seismic hazard levels at the site: 2%, 5%, 10%, and 20% probabilities of exceedance in 50 years (or hazard return periods of 2475, 975, 475, and 224 years, respectively). Each ensemble is comprised of 25 earthquake records for a total of 100 strong ground motions considered in this study. These strong motions were simulated using the Specific Barrier Model (SBM) proposed and developed by Papageorgiou and Aki (1983a, 1983b). This model is based on a stochastic approach for which each earthquake motion is modeled as a spectrum compatible Gaussian noise. The most recent parameters calibrated by Halldorsson (2004) were implemented in the SBM. Figure 2 illustrates various statistical values of the absolute acceleration response spectra at 5% damping for the strong ground motions considered. The 2002 uniform hazard spectra (UHS) obtained from the U.S. Geological Survey (USGS) at the site considered are also shown for comparison purposes. The mean spectral values of the strong ground motions agree well with the 2002 UHS for the range of periods associated with the dynamic characteristics of the structure considered. Details on the generation procedure for the ground motions considered in this study can be found in Wanitkorkul and Filiatrault (2005).

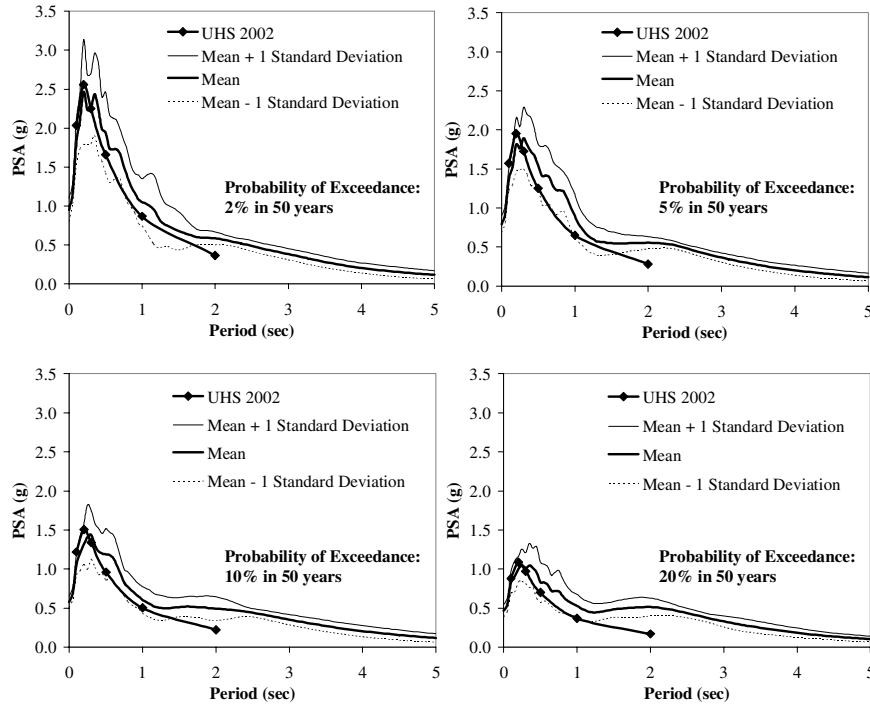


Figure 2. Response spectra of strong ground motion ensembles at 5% damping.

Analysis Results

Structural Fragilities

Computed structural fragilities for the original building and the building retrofitted with hysteretic and viscous dampers against inter-story drifts are shown in Figs. 3 and 4, respectively. The original building fails to achieve the immediate occupancy performance level under all earthquake intensities considered (100% probability of exceeding a drift level of 0.7%). Note that immediate occupancy following a seismic event is highly recommended for this type of acute care facility. On the other hand, all peak inter-story drifts are less than the collapse prevention limit state. Also, for a ground motions corresponding to a return period of 475 years, the probability of exceeding the inter-story drift limit corresponding to the life safety limit state (2.5% drift) is also zero. These results show that this hospital building designed according to the 1970's design requirements would meet the traditional life safety performance level under the 475-year design earthquake but would unlikely remain operational after a design seismic event.

The fragilities against inter-story drifts of the building incorporating hysteretic dampers are much reduced compared to that of the original building. Also the fragilities against inter-story drifts reduce with increasing yield loads of the hysteretic dampers. The peak inter-story drifts are kept below the life safety performance level (2.5% drift) under all earthquake events, except for one of the 2475-year ground motions. However, the incorporation of hysteretic dampers still did not provide a full immediate occupancy performance level for all ground motions. For ground motions having a probability of exceedance of 475 years, for example, the probability of exceeding an inter-story drift level of 0.7% (associated with immediate occupancy) varies from 24% to 56% depending on the yield load level of the dampers, while the corresponding probability value for the original building is 100%. Under all of the 2475-year

ground motions, however, the added hysteretic dampers are not able to prevent the inter-story drifts from exceeding the immediate occupancy drift limit.

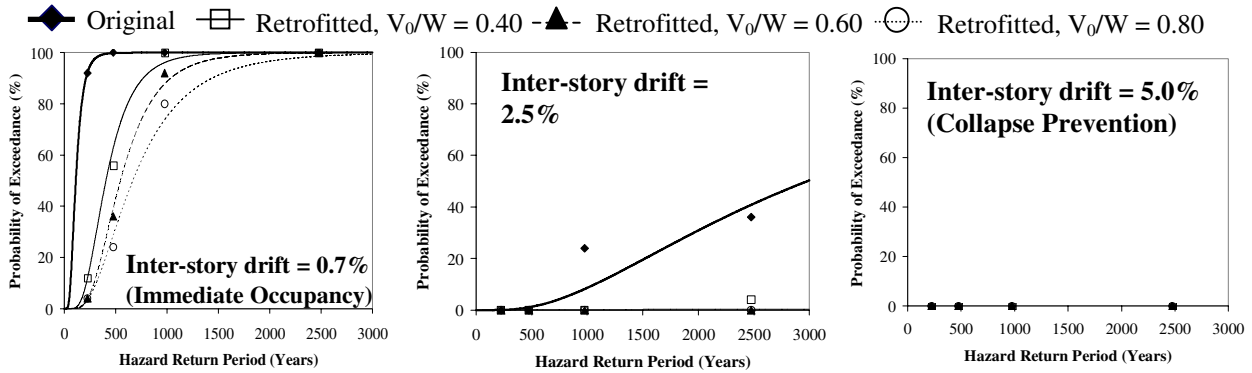


Figure 3. Structural fragilities: Original VS Retrofit with hysteretic dampers

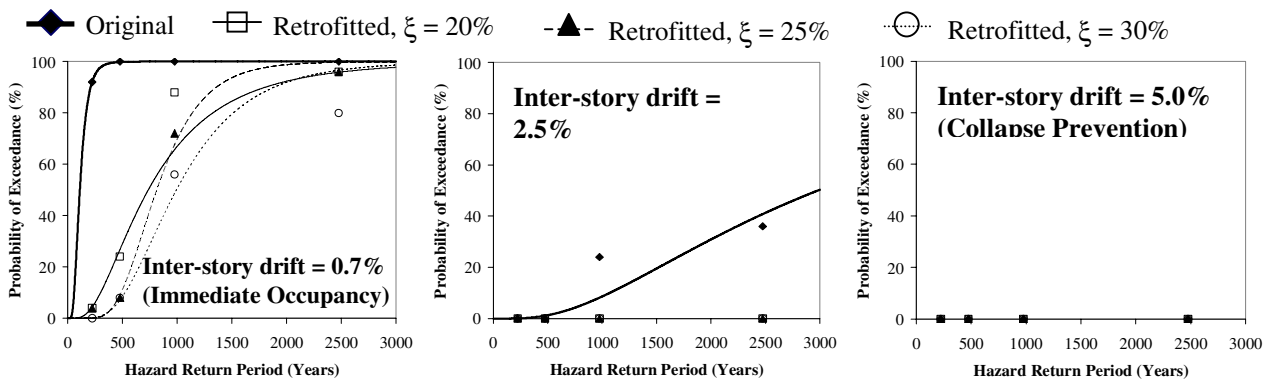


Figure 4. Structural fragilities: Original VS Retrofit with viscous dampers

On the other hand, the results shown in Fig. 4 indicate that the effectiveness of the viscous dampers in reducing the structural fragilities of the building is more pronounced than that of the hysteretic dampers. The fragilities against inter-story drifts are reduced with increasing equivalent viscous damping of the devices. For ground motions having a probability of exceedance of 475 years, for example, the probability of exceeding an inter-story drift level of 0.7% (associated with immediate occupancy) varies from 8% for 30% of equivalent viscous damping to 24% for 20% of equivalent viscous damping, while the corresponding probability value for the original building is 100%. Even under the 2475-year ground motions, the probability of exceeding an inter-story drift level of 0.7% is less than 100%. Also, the incorporation of viscous dampers allows the building to meet the life safety and collapse prevention performance levels under all earthquake excitations.

Nonstructural Fragilities

Figure 5 presents the nonstructural fragilities against absolute accelerations obtained for the three types of nonstructural components considered in the original building. As expected, the nonstructural components located at the roof level of the building exhibit much higher seismic fragilities than those located at the base level. The resonant nonstructural component is the most seismically fragile among the three types of components located on the roof of the building. The resulting peak accelerations of the resonant component are higher than 2.0 g (associated with

moderate damage in this study) for all hazard levels. The probability of exceeding a limit state of 7.0 g (associated with severe damage in this study) is higher than 50% except for the 224-year ground motions. In contrast, when the resonant component is located at the base level, its acceleration fragility is greatly reduced. However, the peak accelerations experienced by the resonant component are still higher than 1.0 g (associated with minor damage) under the 2475-year ground motions and for more than 60% of the 475-year ground motions.

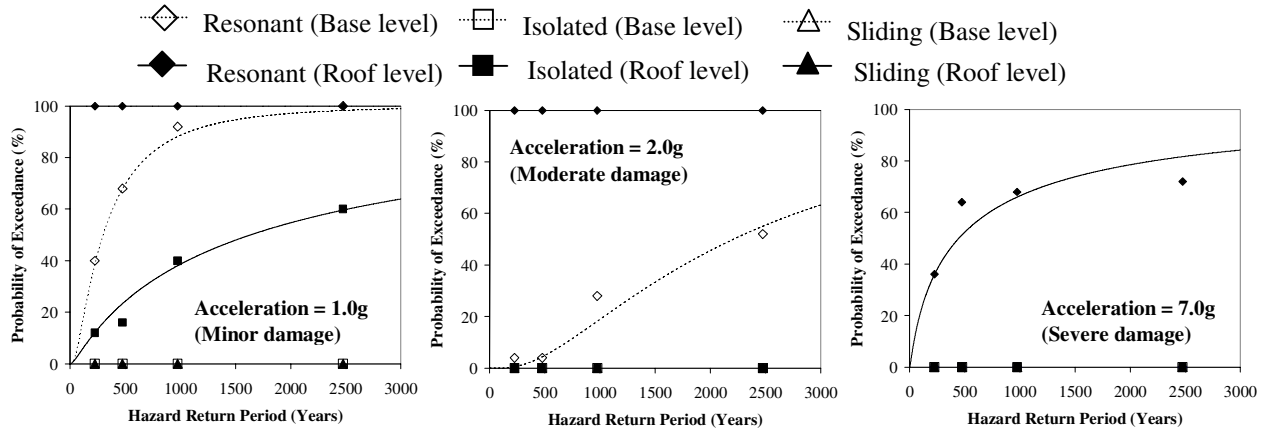


Figure 5. Nonstructural fragilities: Original building

On the other hand, the isolated component, when it is located at the roof level, exhibits much smaller fragility against acceleration response than that of the resonant component. The isolated component undergoes peak acceleration responses mainly between 1.0 g (minor damage) and 2.0 g (moderate damage). The probability that the isolated component located at the roof level exceed an acceleration level of 1.0g varies from 12% for 224-year ground motions to 60% for 2475-year ground motions. All peak accelerations experienced by the isolated component are lower than 1.0g when it is located on the ground level. The results shown also indicate that the sliding nonstructural component located on the roof of the original building exhibits the lowest fragilities among the three types of nonstructural components considered. The acceleration responses of the sliding component are below 1.0g for all ground motions.

For the retrofitted building, since the retrofit strategies have no effect on the responses of the nonstructural components located at the base level, only the fragilities of the nonstructural components located at the roof level of the building are discussed. Figure 6 presents the nonstructural fragilities for building retrofitted with hysteretic dampers. The effectiveness of hysteretic dampers is mixed. For an acceleration level of 1.0 g, for example, the fragility curves for the resonant nonstructural component are essentially unaffected by the presence of hysteretic dampers: in all cases the resonant component fails to meet the minor damage performance level. The effectiveness of the hysteretic dampers improves, however, for the two other performance levels. Also, the incorporation of hysteretic dampers reduces significantly the fragilities of the isolated nonstructural component for all performance levels, including the 1.0g level. For ground motions having a probability of exceedance of 475 years, for example, all isolated components experience peak accelerations less than 1.0 g when hysteretic dampers are incorporated, while the corresponding probability value for the same isolated nonstructural component located on the roof of the original building is 16%. For other performance levels (2.0 g and 7.0 g), the fragility curves shown in Fig. 6 do not allow an evaluation of the effectiveness of hysteretic dampers since in all cases, with and without hysteretic dampers, the performance criteria are met

under all ground motions. A closer review of the results of the dynamic analyses indicates that the incorporation of hysteretic dampers in the building reduces the peak accelerations experienced by the isolated nonstructural components by 8% to 15%. The corresponding reduction in peak accelerations experienced by the sliding nonstructural component is from 1% to 2%.

◆ Original □ $V_n/W = 0.40$ ▲ $V_n/W = 0.60$ ○ $V_n/W = 0.80$

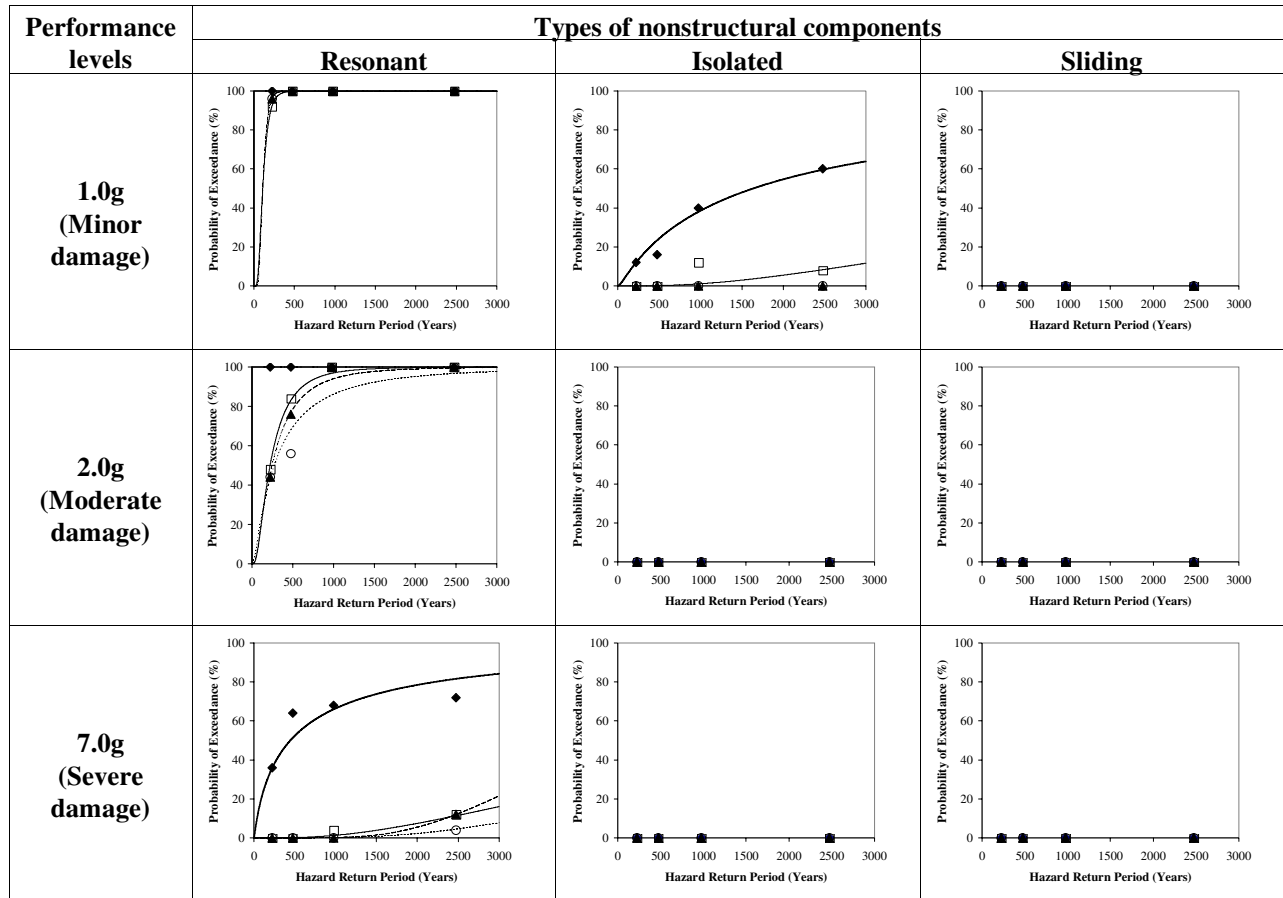


Figure 6. Nonstructural fragilities: Roof level, Retrofit with hysteretic dampers.

The nonstructural fragilities computed for the nonstructural components included in the building retrofitted with viscous dampers are presented in Fig. 7. The results show similar trends as that of hysteretic dampers. Fragilities are reduced with increasing equivalent viscous damping level provided by the viscous dampers. However, the effectiveness of the viscous dampers in reducing nonstructural fragilities is more pronounced than that of hysteretic dampers, especially under the 2475-year earthquake ground motions, which is consistent with the structural fragilities obtained previously.

The results shown in Fig. 7 indicate that even the incorporation of viscous dampers does not allow the resonant component to satisfy the minor damage performance level in terms of peak absolute accelerations (1.0 g level). Similar to the results obtained for hysteretic dampers, the incorporation of viscous dampers is more effective in reducing acceleration fragilities for high performance limits (2.0 g and 7.0 g). For the building retrofitted with viscous dampers

providing a first modal damping ratio of 30% of critical, for example, the probability that the resonant component exceeds a peak absolute acceleration of 2.0 g (associated with moderate damage in this study) is 56% for the 475-year ground motions, while the corresponding probability value for the same resonant component located on the roof of the original building is 100%. The results shown in Fig. 6 clearly show reduced fragilities for the isolated and sliding nonstructural components across performance levels and ground motions.

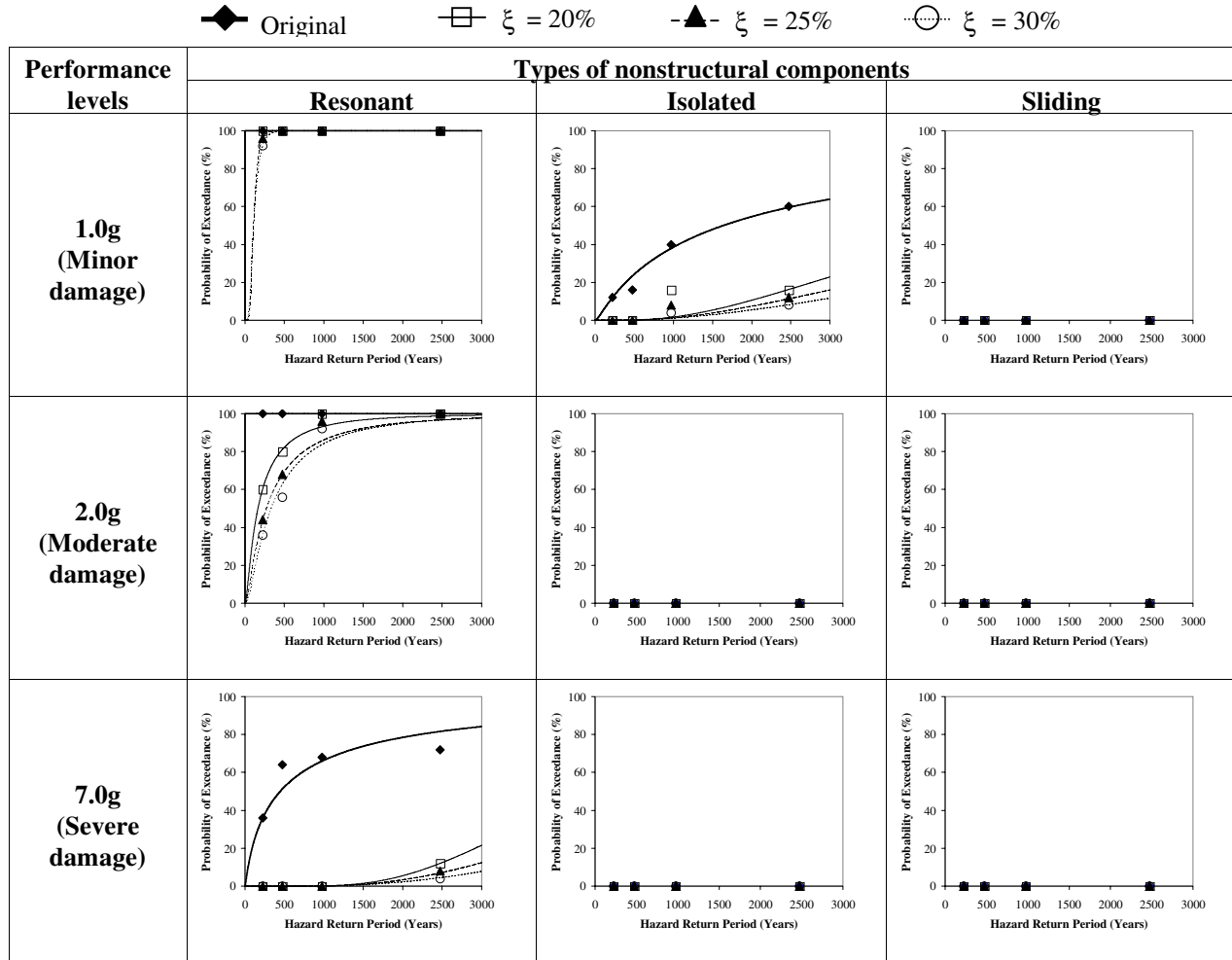


Figure 7. Nonstructural fragilities: Roof level, Retrofit with viscous dampers.

Conclusions

The numerical study described herein investigated the structural and nonstructural fragilities of a building assumed to be part of an acute care facility and incorporating various types of nonstructural components. Based on the results obtained, the following conclusions can be drawn:

- Although the original building met the collapse prevention limit state from an inter-story drift perspective, it failed to achieve the immediate occupancy performance level even under the ground motions corresponding to a return period of only 224 years.

- The hysteretic and viscous damping systems considered in this study have been shown to be effective in reducing the structural fragilities of the building. However the objective of achieving the immediate occupancy performance level was not fully satisfied under the 2475-year ground motions.
- The resonant nonstructural component exhibited the highest fragilities compared to the other two types of nonstructural components considered.
- Isolating technique can effectively reduce accelerations of nonstructural components.
- The sliding nonstructural component exhibited the lowest fragilities among the three types of nonstructural components considered in this study, however; in practical applications, restraining systems may be needed to prevent impacts between adjacent sliding equipment.
- The resonant nonstructural component was more sensitive to the retrofit system incorporated to the building, while less effect was observed for the other two types of nonstructural components.
- Retrofitting the building with viscous dampers proved to be more efficient in reducing the fragilities against floor and nonstructural components accelerations than that of hysteretic dampers.

Acknowledgements

This work was supported primarily by the Earthquake Engineering Research Centers Program of the National Science Foundation under NSF Award Number EEC-9701471 to the Multidisciplinary Center for Earthquake Engineering Research. Any opinions, findings and conclusions or recommendations expressed in this material are those of the author(s) and do not necessarily reflect those of the National Science Foundation.

References

- Applied Technology Council (ATC), 2000. *NEHRP Guidelines for the Seismic Rehabilitation of Buildings, Federal Emergency Management Agency (FEMA 354)*, Washington D.C.
- Filiatrault, A., Tremblay, R., and Wanitkorkul, A., 2001. Performance Evaluation of Passive Damping Systems for the Seismic Retrofit of Steel Moment Resisting Frames Subjected to Near Field Ground Motions, *Earthquake Spectra* 17 (3), 427-456.
- Halldorsson, B., 2004. Calibration of the Specific Barrier Model to Earthquakes of Different Tectonic Regions and the Synthesis of Strong Ground Motions for Earthquake Engineering Applications, *Ph.D. Dissertation*, Dept. of Civil, Structural, and Environmental Engineering, University at Buffalo, State University of New York, Buffalo, NY.
- International Conference of Building Officials (ICBO), 1970. *Uniform Building Code, 1970 Edition*, Whittier, CA.
- Papageorgiou, A.S. and Aki, K., 1983a. A Specific Barrier Model for the Quantitative Description of Inhomogeneous Faulting and the Prediction of Strong Ground Motion, Part I: Description of the Model, *Bull. Seism. Soc. Am.* 73, 693-722.
- Papageorgiou, A.S. and Aki, K., 1983b. A Specific Barrier Model for the Quantitative Description of Inhomogeneous Faulting and the Prediction of Strong Ground Motion, Part II: Applications of the Model, *Bull. Seism. Soc. Am.* 73, 953-978.
- Wanitkorkul, A. and Filiatrault, A., 2005. Simulation of Strong Ground Motions for Seismic Fragility Evaluation of Nonstructural Components in Hospitals, *Technical report MCEER-05-0005*, Multidisciplinary Center for Earthquake Engineering Research, University at Buffalo, State University of New York, Buffalo, NY.